

PNNL-38277

Demonstration of Optical Spectroscopic Flow Cell Design for Molten Salt Reactor Off-Gas Streams

September 2025

Heather M. Felmy
Poki Tse
Paulina Guerrero-Almaraz
Samuel A. Bryan
Amanda M. Lines



U.S. DEPARTMENT
of ENERGY

Prepared for the U.S. Department of Energy
under Contract DE-AC05-76RL01830

DISCLAIMER

This report was prepared as an account of work sponsored by an agency of the United States Government. Neither the United States Government nor any agency thereof, nor Battelle Memorial Institute, nor any of their employees, makes **any warranty, express or implied, or assumes any legal liability or responsibility for the accuracy, completeness, or usefulness of any information, apparatus, product, or process disclosed, or represents that its use would not infringe privately owned rights.** Reference herein to any specific commercial product, process, or service by trade name, trademark, manufacturer, or otherwise does not necessarily constitute or imply its endorsement, recommendation, or favoring by the United States Government or any agency thereof, or Battelle Memorial Institute. The views and opinions of authors expressed herein do not necessarily state or reflect those of the United States Government or any agency thereof.

PACIFIC NORTHWEST NATIONAL LABORATORY
operated by
BATTELLE
for the
UNITED STATES DEPARTMENT OF ENERGY
under Contract DE-AC05-76RL01830

Printed in the United States of America

Available to DOE and DOE contractors from
the Office of Scientific and Technical Information,
P.O. Box 62, Oak Ridge, TN 37831-0062

www.osti.gov
ph: (865) 576-8401
fox: (865) 576-5728
email: reports@osti.gov

Available to the public from the National Technical Information Service
5301 Shawnee Rd., Alexandria, VA 22312
ph: (800) 553-NTIS (6847)
or (703) 605-6000
email: info@ntis.gov
Online ordering: <http://www.ntis.gov>

Demonstration of Optical Spectroscopic Flow Cell Design for Molten Salt Reactor Off-Gas Streams

September 2025

Heather M. Felmy
Poki Tse
Paulina Guerrero-Almaraz
Samuel A. Bryan
Amanda M. Lines

Prepared for
the U.S. Department of Energy
under Contract DE-AC05-76RL01830

Pacific Northwest National Laboratory
Richland, Washington 99354

Summary

Molten salt reactors (MSRs) represent a powerful opportunity to meet the growing energy needs in the United States while offering improved efficiency and safety as compared to the existing fleet. To better enable and support industry efforts in these areas, national laboratories can advance key technologies to support the deployment and operation of these reactors. A key example of this is advancing the off-gas management systems.

Advancement and integration of on-line monitoring tools can be particularly beneficial as it can support needs at multiple stages. For example, integration of probes and sensors that can provide *in situ* and real-time characterization of the off-gas line and enable more efficient and informed development and optimization of treatment systems. On-line monitoring tools can also support scale up and ultimately cost-effective deployment of treatment systems.

PNNL has been developing and demonstrating Raman-based monitoring sensors that can identify and quantify multiple polyatomic species simultaneously. Examples include various iodine species, multiple hydrogen isotopologues, and contaminants such as O₂ and N₂. Efforts have involved advancing gas sensor flow cells to improve sensitivity for key analytical targets, developing automated data-science tools for real-time translation of Raman spectra to analyte concentrations, and validation of sensor performance on real flow loops. Progress in FY25 has been notable, with the key highlights of:

- 1) In collaboration with ORNL, PNNL integrated 4 Raman sensors onto the Facility to Alleviate Salt Technology Risks (FASTR) loop at ORNL. This was a coordinated effort to integrate multiple complementary sensors onto the loop and provided a valuable demonstration of interlab collaboration and comprehensive characterization of off-gas streams.
- 2) The Raman sensor flow cell was further optimized to improve sensitivity for target analytes while eliminating non-beneficial components to improve simplicity of installation. Improved performance as compared to standard gas probes was demonstrated on the ORNL FASTR loop. Off-loop H₂ and D₂ measurements demonstrated a lower limit of detection (LOD) than previous measurements on standard Raman probes.

Overall results demonstrate the development and maturation of technologies that can directly support the advancement and deployment of molten salt reactor off-gas treatment systems. Furthermore, results suggest that expansion of connected and complimentary sensor measurements can provide the comprehensive level of information needed by both researchers and operators to support MSR needs. Submission of this report meets milestone M3AT-25PN0702061: "Complete demonstration of flow cell design on representative gas stream."

Acknowledgments

This work was funded by U.S. Department of Energy, Office of Nuclear Energy, through the Advanced Reactor Technology Program and was performed at Pacific Northwest National Laboratory (PNNL) operated by Battelle for the U.S. Department of Energy under contract DE-AC05-76RL01830. The PNNL team would like to thank Kevin Robb, Hunter Andrews, Joanna McFarlane, Zechariah Kitzhaber, and Daniel Orea for all their help with the onsite demo at ORNL.

Acronyms and Abbreviations

CCD	Charge-coupled device
COTS	commercial off the shelf
DOE	Department of Energy
FASTR	Facility to Alleviate Salt Technology Risks
LIBS	laser-induced breakdown spectroscopy
LOD	Limit of detection
LSTL	liquid salt test loop
MSR	Molten salt reactors
NE	Nuclear Energy
NRC	Nuclear Regulatory Commission
ORNL	Oak Ridge National Laboratory
PNNL	Pacific Northwest National Laboratory
RGA	residual gas analyzer
TRL	technology readiness level

Contents

Summary	iii
Acknowledgments.....	iv
Acronyms and Abbreviations.....	v
1.0 Introduction	1
2.0 Instrumentation and sensor development.....	3
2.1 Improving instrumentation.....	3
2.1.1 Initial aqueous testing of instrumentation.....	4
2.2 Improving sensor design	5
3.0 Demonstration at ORNL	7
3.1 Onsite demo at ORNL.....	7
3.1.1 Instrumentation.....	7
3.1.2 Demo results	7
4.0 Conclusions and recommendations.....	16
5.0 References.....	17

Figures

Figure 1.	Photo of new Raman instrument on a cart with a laptop to operate the instrument.	3
Figure 2.	Comparison of Raman signal and LODs for solutions of 0 – 6 M NaNO ₃ for the A) new instrument and B) old instrument along with the C) corresponding calibration curves.....	4
Figure 3.	Raman probe with A) a short barrel and B) a long barrel.....	5
Figure 4.	A) N ₂ Raman measurement in air of each collection port of the FY24 gas cell. B) Schematic of FY24 gas cell showing location of 4 collection ports. C) Photo of FY24 gas cell.	6
Figure 5.	A) Schematic of FY25 gas flow cell. B) Photo of FY25 gas flow cell.....	6
Figure 6.	A) PNNL and ORNL team members who participated in the demo at ORNL. B) LIBS and Raman team members collecting measurements.....	8
Figure 7.	D ₂ measurement setup for comparison of Raman probe and gas flow cell.....	8
Figure 8.	Raman measurement of 4% D ₂ in Ar comparing a traditional Raman probe to the gas flow cell collected at A) 20 second integration and B) 60 second integration time.	9
Figure 9.	Raman calibration measurements of 0 – 20 psig (0 – 41 Torr) of A) D ₂ and B) H ₂ along with the corresponding calibration curves and LODs for C) D ₂ and D) H ₂	10
Figure 10.	A) Schematic of FASTR adapted from a previous report ¹⁶ with Raman probe locations indicated in orange (not to scale). Photos of locations	

	where Raman probes were incorporated into the FASTR loop are shown in B) salt storage tank, C) pump tank, D) top of the manifold.....	11
Figure 11.	Top-down surface plots of Raman spectra measured on the Raman probe above the salt storage tank highlighting the A) D ₂ region, B) HD region, and C) H ₂ region. D) Peak intensities for D ₂ , HD, and H ₂ . E) Flow rates of H ₂ and D ₂ gas sparging. Spectra were averaged using a moving mean of 19 points.	12
Figure 12.	A) LIBS, RGA, and Raman instrumentation arranged for simultaneous measurements. B) Sampling of gas line from salt storage tank for simultaneous RGA, Raman, and LIBS measurements.	13
Figure 13.	Top-down surface plots of Raman spectra collected on the Raman probe above the salt storage tank highlighting the A) D ₂ region, B) HD region, and C) H ₂ region. D) Peak intensities for D ₂ , HD, and H ₂ . E) Flow rates of H ₂ and D ₂ gas sparging. Spectra were averaged using a moving mean of 19 points.	14
Figure 14.	Top-down surface plots of Raman spectra collected on the gas flow cell highlighting the A) D ₂ region, B) HD region, and C) H ₂ region. D) Peak intensities for D ₂ , HD, and H ₂ . E) Flow rates of H ₂ and D ₂ gas sparging. Spectra were averaged using a moving mean of 19 points.	15

1.0 Introduction

MSRs have been recognized as a key next generation nuclear reactor technology that can safely and efficiently provide energy. Several reactor designers are advancing this technology, with some in the process of building test reactors (e.g. TerraPower) or pursuing NRC licensing (Kairos). Notably, MRSS can come in a variety of forms with a general commonality being off-gas treatment systems. These treatment systems and the need they fill have been covered in detail elsewhere.¹⁻³

A key item to note is the benefit of including on-line monitoring tools through the design, optimization, scale up, and deployment of these off-gas treatment systems. On-line monitoring, or the integration of sensors directly on process lines to support *in situ* and real-time process characterization, can drastically accelerate and reduce costs of deployment. For the development of off-gas treatment systems starting at lower technology readiness levels (TRLs), on-line monitoring can provide researchers with real-time feedback regarding system modifications and optimizations. When pushing to higher TRLs, a key example being going through the scale up process, on-line monitoring can provide insight that allows engineers to more efficiently modify the system while reaching performance targets. At high TRLs (deployment of treatment systems) on-line monitoring offers operators a powerful tool for real-time process control. Ultimately, this can reduce grab sample costs, avoid upsets, and maintain optimal operational conditions.

For MSR off-gas treatment systems where chemical constituency is complex and the measurement environment is damaging towards sensor equipment (e.g. through corrosivity or radiation), there are often no sensors commercially available that can be readily deployed. This is true from both a material performance standpoint (i.e. sensors on the market are not designed from materials hardened for radiation or chemical corrosivity) or from an automated data analysis standpoint (i.e. there are no plug and play tools that can allow sensors to translate raw data into useful information for operators within these complex chemical environments). To enable the MSR industry to realize the benefits of on-line monitoring, it is essential that these tools be developed and advanced in TRL along with gas treatment technology.

Many sensors could ultimately be valuable in off-gas treatment systems, but a key component will need to be optical sensors due to their unique ability to provide detailed insight into chemical compositions and concentrations. Furthermore, for comprehensive characterization, integrating multiple types of probes will allow for characterization of the full suite of target analytes of interest. Key examples of applicable optical tools for MSR off-gas include Raman^{4, 5} and laser-induced breakdown spectroscopy (LIBS).⁶⁻⁸ These tools provide highly complementary information, where Raman can characterize molecular species and LIBS can characterize elemental species.

Under DOE-NE funding, Raman and LIBS tools have been advanced for MSR off-gas applications. This has been a collaborative effort between Pacific Northwest National Laboratory (PNNL), and Oak Ridge National Laboratory (ORNL), where PNNL has focused on Raman and ORNL has focused on LIBS. Under previous work, PNNL has demonstrated Raman applicability to various off-gas species of interest, including iodine species and hydrogen isotopologues.⁹⁻¹¹ Most notably this previous work highlights efforts to both optimize sensors for off-gas systems as well as develop automated, data-science based tools for real-time data analysis.

In addition to being able to simultaneously identify and quantify a wide range of molecular species of interest within off-gas treatment systems, Raman has demonstrated a number of other benefits of application. Probes and sensor flow cells can be fabricated out of materials that can withstand the corrosive environment and do not contain electronics, making them ideal for applications

within radioactive environments. Additionally, probes connect to instrumentation via fiber optics which can be 100's m long,¹² meaning all the sensitive components can be well outside of the process hazard zone. Raman is also a highly mature technology, where instrumentation is widely commercially available. A key note, while historically it has been difficult to procure probe components needed for off-gas systems commercial off the shelf, PNNL's work with small business partners has resulted in off-gas-applicable sensors now being more easily available.

Recent work has been focused on addressing challenges in two key areas:

- 1) Improving sensitivity for low concentration species (tritium is a key example of an important analytical target)
- 2) Demonstrating Raman performance and ability to be integrated into operating off-gas loops
 - a. With a key aspect being demonstrating complimentary and simultaneous operation with additional sensors (e.g. LIBS) for comprehensive gas characterization

This report will cover the results of FY25 efforts to address points 1 and 2 above. Specifically, the design and testing of new, optimized Raman flow cells for gas analysis will be discussed. Results indicate improved performance, and the more streamlined flow cell footprint lends itself to easier installation. Additionally, efforts to complete an on-site demonstration of Raman on an active salt loop at ORNL will be discussed. This highly successful deployment was completed through close collaboration with the ORNL team and results indicate not only good performance of Raman, but highly beneficial connection between multiple sensors simultaneously operating on the loop.

Overall, Raman continues to demonstrate that it is a key component of a complete on-line monitoring portfolio to support development and deployment of MSR off-gas treatment systems.

2.0 Instrumentation and sensor development

Gas-phase measurements performed in previous FYs have utilized existing instrumentation and sensors which were not specifically designed for gas-phase measurements. A key aspect of this work was procuring instrumentation and sensors with specifications designed to improve signal for gas-phase species.

2.1 Improving instrumentation

A new Raman instrument (Spectra Solutions) was purchased for this work and includes specifications for gas-phase measurements. Previous work has demonstrated that lower wavelength, higher energy excitation lasers provide increased signal.¹¹ Based on this previous experience, the new instrument was designed to include 60 mW 406 nm (blue) lasers and a back illuminated charge-coupled device (CCD) detector with a usable range up to 5000 cm^{-1} to cover the range of all hydrogen isotopologues (up to 4160 cm^{-1} for H_2). The new instrument is also a 6-track instrument, meaning that signal from 6 collection ports can be collected simultaneously. This allows for 6 different measurement locations. Each track has its own excitation laser excitation, and the laser light is transmitted to the sensor via fiber optic cables. The scattered light will be transmitted back to the corresponding detector track. Figure 1 shows a photo of the new Raman instrument with fiber optical cables attached to several of the excitation and collection ports. These fiber optic cables can be manufactured to be very long (up to hundreds of meters¹²) and therefore allow the instrument and operators to reside far away from the sensor. This not only adds convenience for instrument placement but also improves safety by adding distance from high temperature or radiation environments.

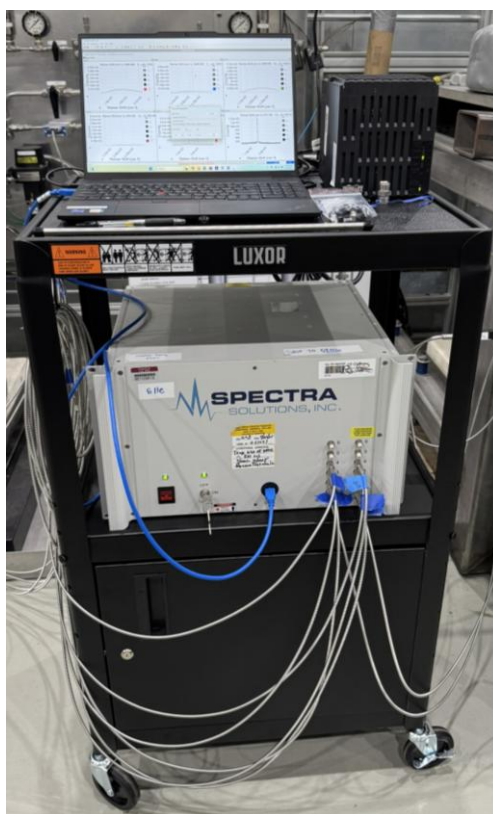


Figure 1. Photo of new Raman instrument on a cart with a laptop to operate the instrument.

2.1.1 Initial aqueous testing of instrumentation

Initial testing of the new instrument was done in aqueous systems for ease of sample preparation and measurement. A series of aqueous solutions were prepared to compare the performance of the existing 405 nm Raman system to the new 406 nm Raman system. Thirty-five samples with various concentrations of sodium nitrate, sodium chloride, and nitric acid were prepared to evaluate the change in the nitrate peak from two different nitrate sources. Adding sodium chloride was used to evaluate the ionic strength effect on the nitrate peak. The samples were measured in a 1 cm pathlength glass cuvette with a cuvette holder capable of aligning the Raman probe. The samples were measured on both the old 405 nm and new 406 nm Raman systems at an integration time of 0.2 s. An example of the aqueous testing results is shown in Figure 2 for solutions of NaNO_3 . The NO_3^- peak intensity at 1050 cm^{-1} was compared between both the old and new Raman instrument and the LOD was calculated for each instrument. The equation used to calculate the limit of detection is shown in Equation 1, where s is the standard deviation of a blank measurement (water), and m is the slope of the calibration curve.

$$LOD = 3s/m \quad (1)$$

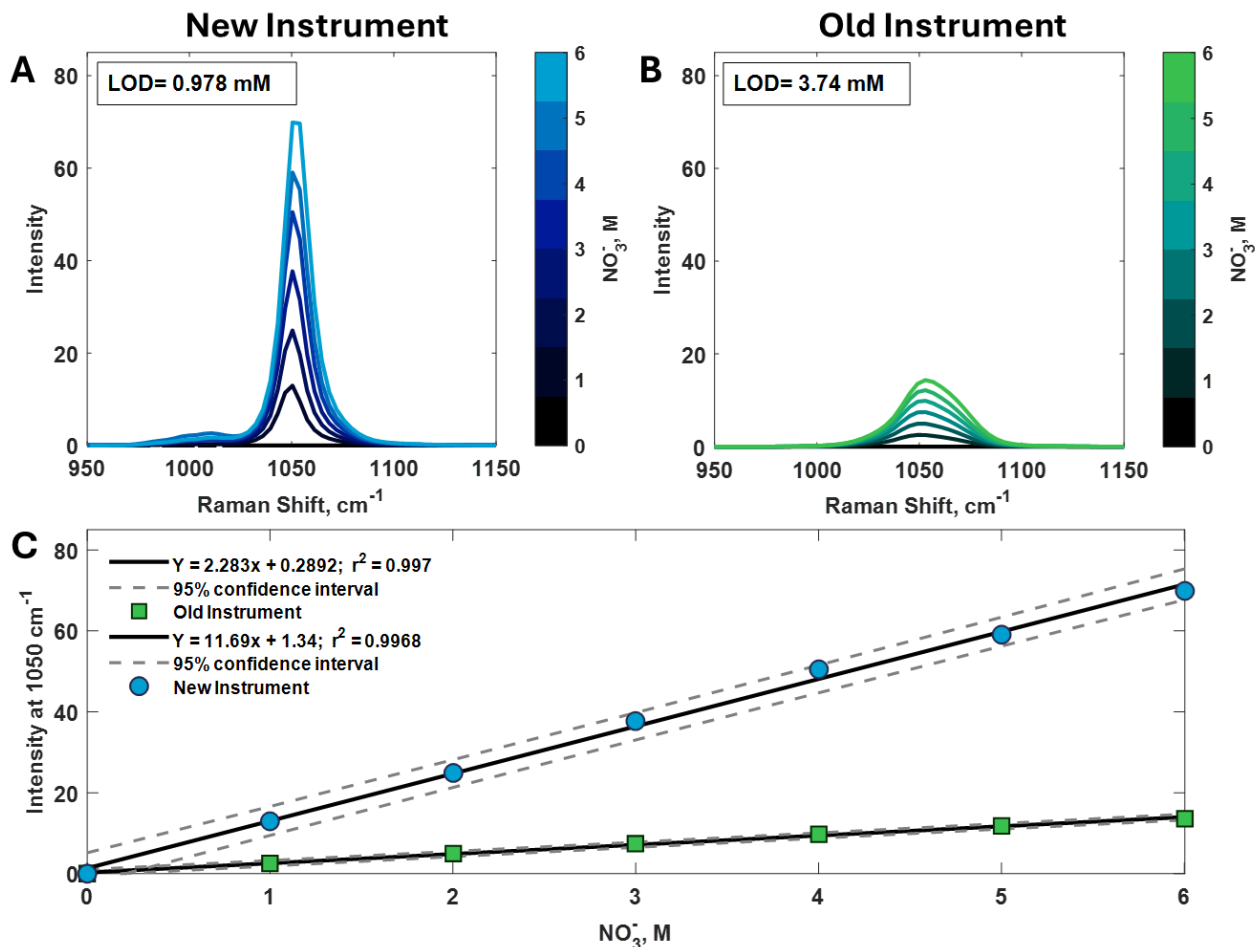


Figure 2. Comparison of Raman signal and LODs for solutions of 0 – 6 M NaNO_3 for the A) new instrument and B) old instrument along with the C) corresponding calibration curves.

The LOD of nitrate on the new instrument was more than 3 times lower than the LOD of the old instrument and the new instrument had more than 5 times higher signal than the old instrument. While these aqueous results may not translate exactly to gas-phase measurements, as detector sensitivity varies across the spectrum, these are very promising results and indicate that the new instrument is more sensitive than the old instrument.

2.2 Improving sensor design

Another aspect of ongoing work is improving the design of the Raman sensors. Traditional Raman probes consist of a probe body connected to fiber optic cables and a probe barrel with a focusing lens. These barrels can be manufactured at various lengths, with different focal lengths, and constructed out of different materials. Two probes with different barrel sizes are shown in Figure 3. This Raman probe design is commercial off the shelf (COTS), customizable, and can be easily incorporated into a process by either shining the laser through an optically transparent window or by immersing the end of the barrel directly into the process line. While there are advantages to using these COTS probes, new designs of gas measurement cells were explored with the goal of improving sensitivity and LODs.

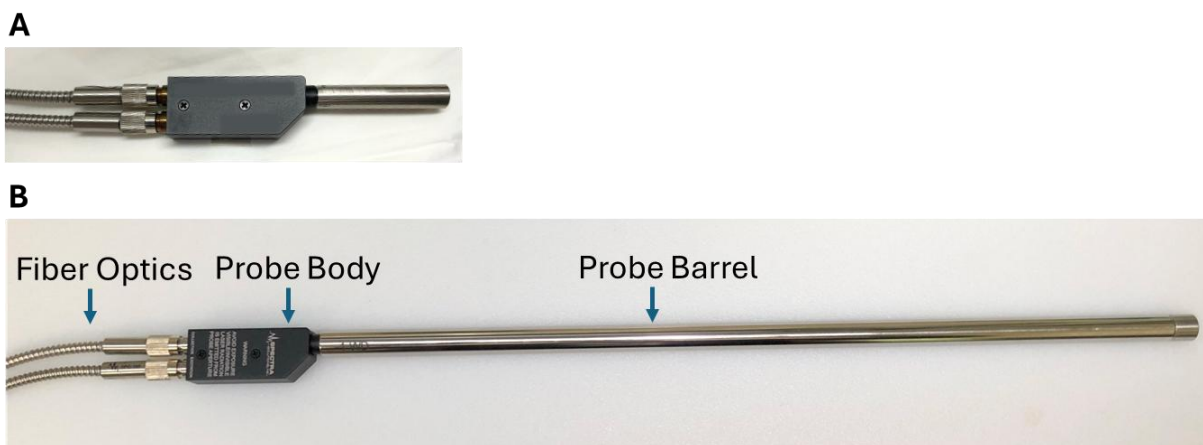


Figure 3. Raman probe with A) a short barrel and B) a long barrel.

In FY24, a new gas cell was designed which consisted of a Raman probe body attached to a cell with 3 additional collection ports. This design improved the Raman signal over the single barrel design. Figure 4 shows a photo and schematic of the FY24 gas cell design. This cell was tested in air by following the peak intensity of N_2 . This test was done where only one collection fiber was attached at a time, and the Raman signal of N_2 was measured. The results are shown in Figure 4A where it was determined that a majority of the Raman signal was collected on the fiber attached directly to the Raman probe and the one that was 180° from the Raman probe. This inspired a new design in FY25.

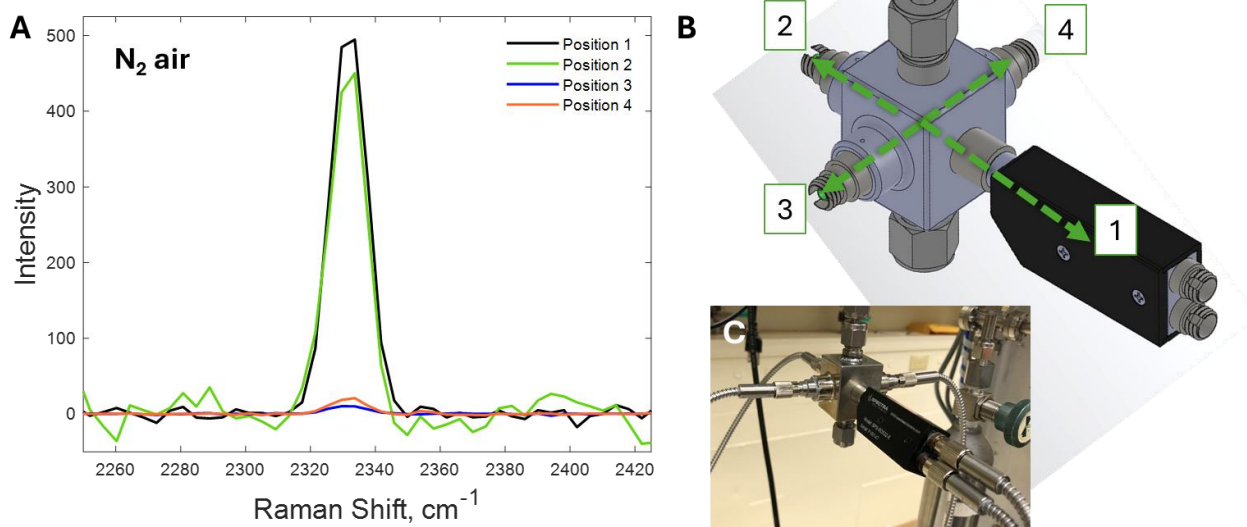


Figure 4. A) N₂ Raman measurement in air of each collection port of the FY24 gas cell. B) Schematic of FY24 gas cell showing location of 4 collection ports. C) Photo of FY24 gas cell.

The FY25 gas flow cell was designed to take advantage of the increased signal from the FY24 design but in a simpler form. Instead of a second collection port opposite the Raman probe, a mirror was added to reflect the signal back to the Raman probe body. A schematic and photo of the gas flow cell are shown in Figure 5. With this design, only one collection port on the probe body is required, which would allow for multiple gas flow cells to be used simultaneously. The new Raman instrument would be capable of collecting data on up to 6 gas flow cells if desired. Results using the FY25 gas cell are reported in Section 3.

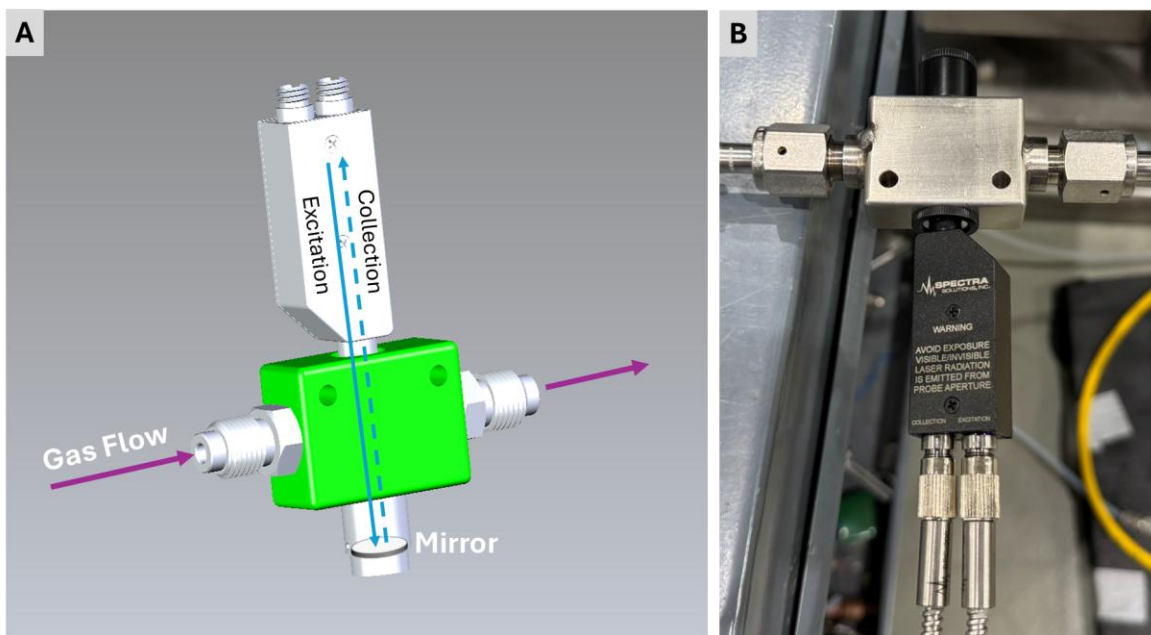


Figure 5. A) Schematic of FY25 gas flow cell. B) Photo of FY25 gas flow cell.

3.0 Demonstration at ORNL

PNNL has maintained an ongoing collaboration with ORNL. This has involved sensor testing during previous FASTR and liquid salt test loop (LSTL) runs as well as preparation and finally completing a demo of combined sensors on FASTR. This demo was a unique opportunity for the deployment of multiple sensors on a salt loop. The teams were able to measure Raman in tandem with residual gas analyzer (RGA) and LIBS for a demonstration of the benefits and needs for online monitoring in multiple forms.

During previous runs on FASTR and LSTL, PNNL shipped Raman probe barrels to ORNL to incorporate into the loops. These barrels were inserted into the loops to test the survivability of the sensors. The results were presented in the FY24 report.¹³ Most of the probes did survive the testing with only minor discoloration due to heat exposure.

3.1 Onsite demo at ORNL

3.1.1 Instrumentation

The newly acquired PNNL Raman spectrometer described in Section 2.1 was shipped to ORNL for the demonstration on the salt loop. Fiber optic cables (15 – 20 m length) connected this instrument to 4 Raman sensors incorporated into the loop. These sensors included 3 traditional Raman probes and the newly designed gas flow cell.

The ORNL instrumentation included RGA and LIBS. For these experiments, an RGA sampling line was attached in line with Raman and LIBS to provide tandem mass spectrometry results of the gas phase. The LIBS sensor for monitoring aerosol/gas phases setup for this study used a mobile LIBS platform with a modular design, allowing various sample stream configurations and spectrometers.^{14, 15} Two spectrometers were used: a multichannel spectrometer with broad elemental coverage (6-channel 4096CL, Avantes) and a high-resolution spectrometer with narrow bandwidth (~2 nm) but capable of resolving isotopic shifts (DEMON, Lasertechnik Berlin). Both the DEMON spectrometer and LIBS platform were outfitted on separate carts for transportation between laboratories.

3.1.2 Demo results

In August 2025, three members of the PNNL team (Paulina Guerrero-Almaraz, Heather Felmy, and Sam Bryan) traveled to ORNL for a weeklong demonstration at ORNL. During this demo, the PNNL Raman system was able to collect data from 3 Raman probes similar to the one pictured in Figure 3B, as well as the newly acquired FY25 gas flow cell pictured in Figure 5B. The PNNL and ORNL team members participating in the demo are pictured in Figure 6A and Figure 6B shows some of the LIBS and PNNL team members operating the instrumentation next to the FASTR loop.

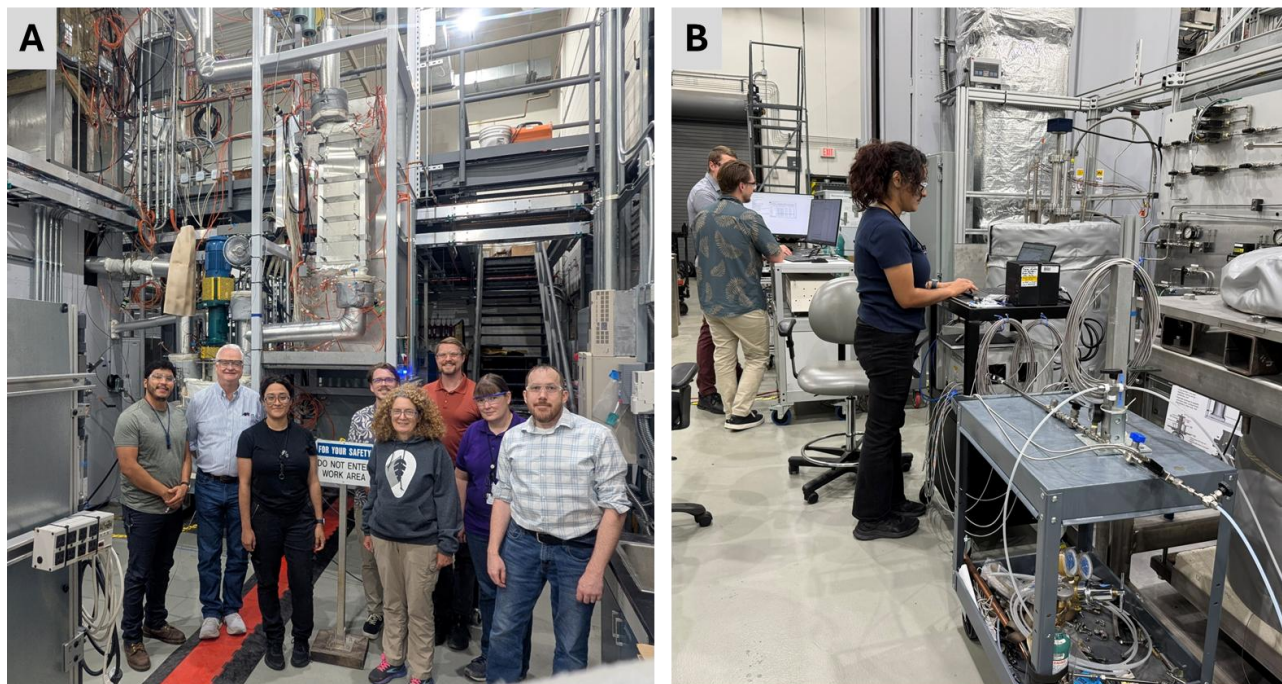


Figure 6. A) PNNL and ORNL team members who participated in the demo at ORNL. B) LIBS and Raman team members collecting measurements.

Initial studies were conducted outside of the salt loop for comparison of Raman sensors. Figure 7 shows a gas line with a Raman probe and gas flow cell attached to the same gas space. This gas line was filled with 4% D_2 in Ar and the probe signals were compared.

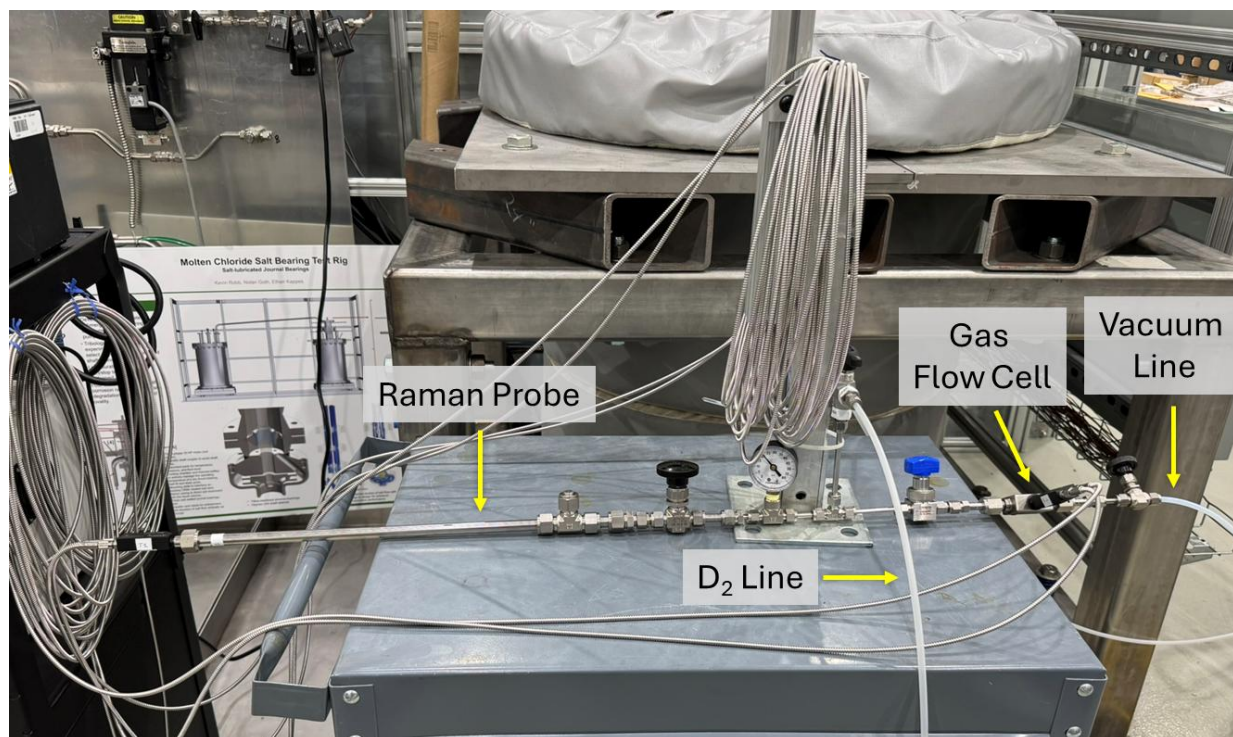


Figure 7. D_2 measurement setup for comparison of Raman probe and gas flow cell.

Figure 8 shows the results of the gas flow cell and Raman probe measurements of 4% D₂ in Ar. The data shown includes two different integration times. The integration time, or the time that Raman signal is collected for a single spectrum, can be optimized for each experiment. The longer the integration time, the higher the signal, but longer integration times mean fewer spectra can be collected over a given period of time and quicker reactions can be missed. From Figure 8, the gas flow cell produced a much higher signal than the Raman probe. All additional experiments utilized an integration time of 20 seconds in order to monitor for faster changes in the system. Additional post-processing of data including spectral averaging was performed on the measurements to improve signal for both the Raman probe data and the gas flow cell data.

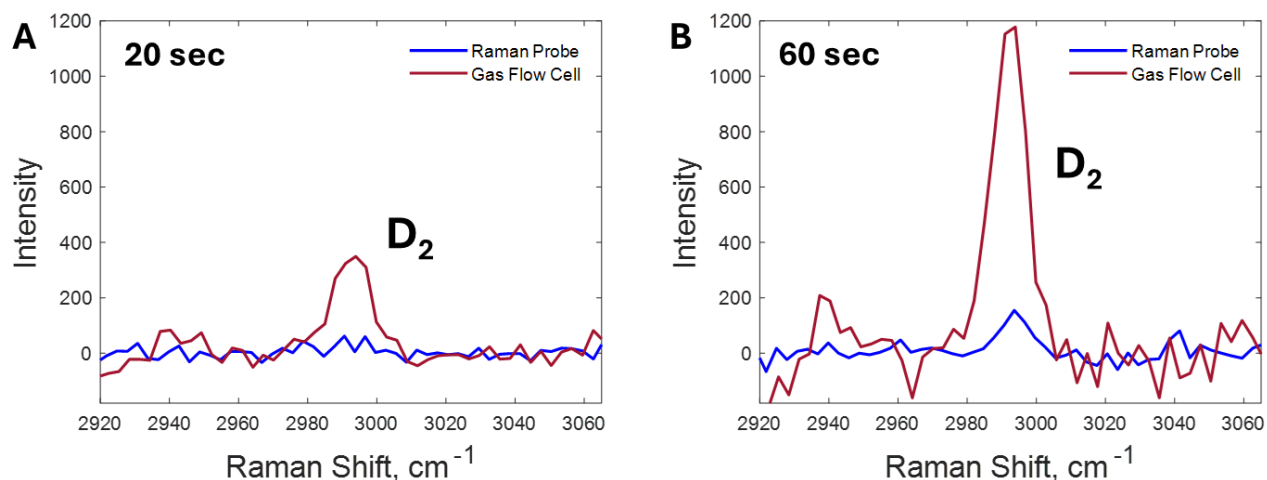


Figure 8. Raman measurement of 4% D₂ in Ar comparing a traditional Raman probe to the gas flow cell collected at A) 20 second integration and B) 60 second integration time.

Estimated calibration curves for Raman were developed for D₂ and H₂ measured on the gas flow cell. Raman, RGA, and LIBS were measured simultaneously and will be compared in future work. The concentration range was limited to up to 4% H₂ or D₂ in Ar for safety requirements. The results are shown in Figure 9. For these measurements, 0 – 20 psig (0 – 41 Torr) D₂ or H₂ was flowed through the Raman gas flow cell. The pressures were measured at the tank, not the measurement location, so exact gas pressures in the measurement cell are expected to be slightly different. Despite this, there was a noticeable trend of peak intensity versus gas pressure. From this, an estimated LOD was calculated as 5 Torr for D₂ and 3.8 Torr for H₂. These were lower LODs than previously measured on the older Raman system with a traditional Raman probe which were 10.0 Torr for D₂ and 13.1 Torr for H₂.¹¹ Additional calibration measurements are planned to get a better LOD determination.

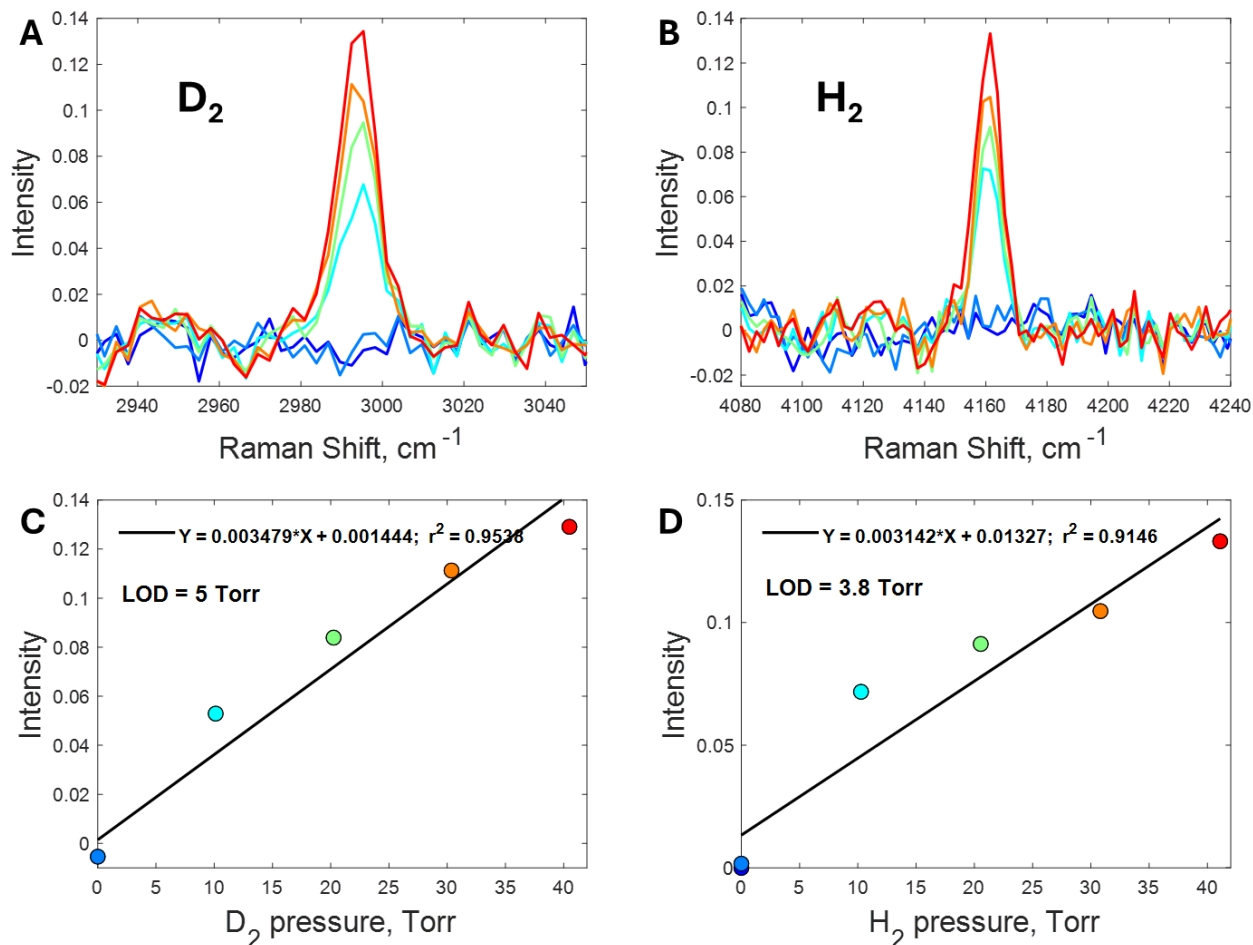


Figure 9. Raman calibration measurements of 0 – 20 psig (0 – 41 Torr) of A) D_2 and B) H_2 along with the corresponding calibration curves and LODs for C) D_2 and D) H_2 .

For the Raman measurements performed on the FASTR loop, Raman probes were attached in 3 locations which are shown in Figure 10 in both a schematic of the loop and photos of the probe locations. These locations were chosen to encompass much of the gas phase portions of the loop. These probes were installed at the start of the demo and collected data for much of the weeklong experiment. These probes will be shipped back to PNNL after the end of the salt loop run for characterization and to determine if any damage was sustained from heat or corrosion.

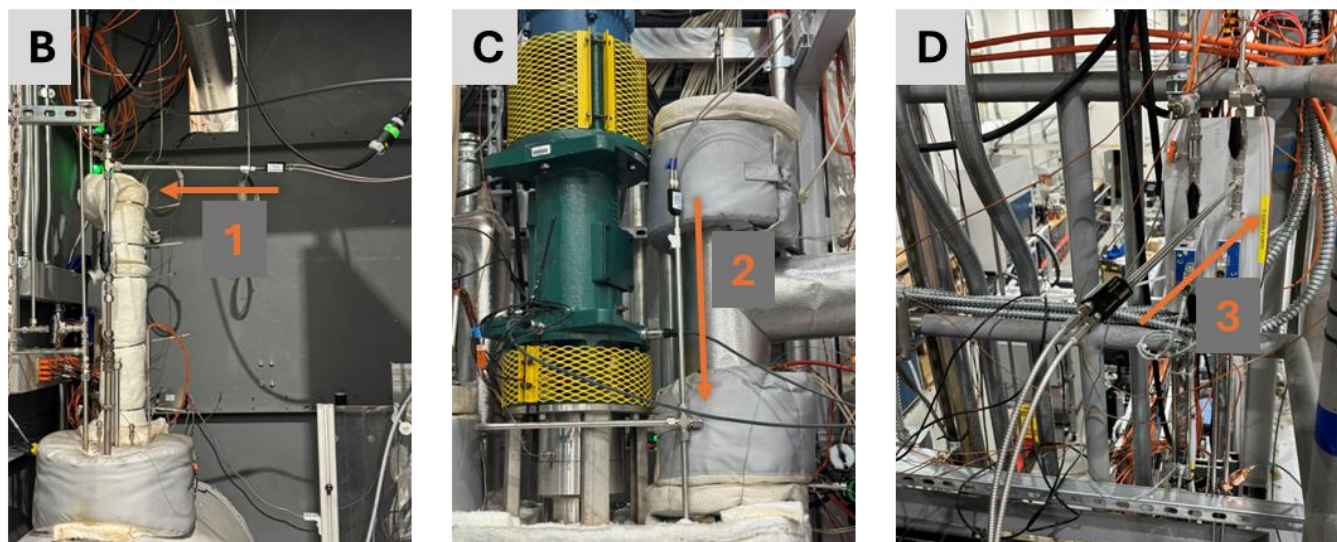
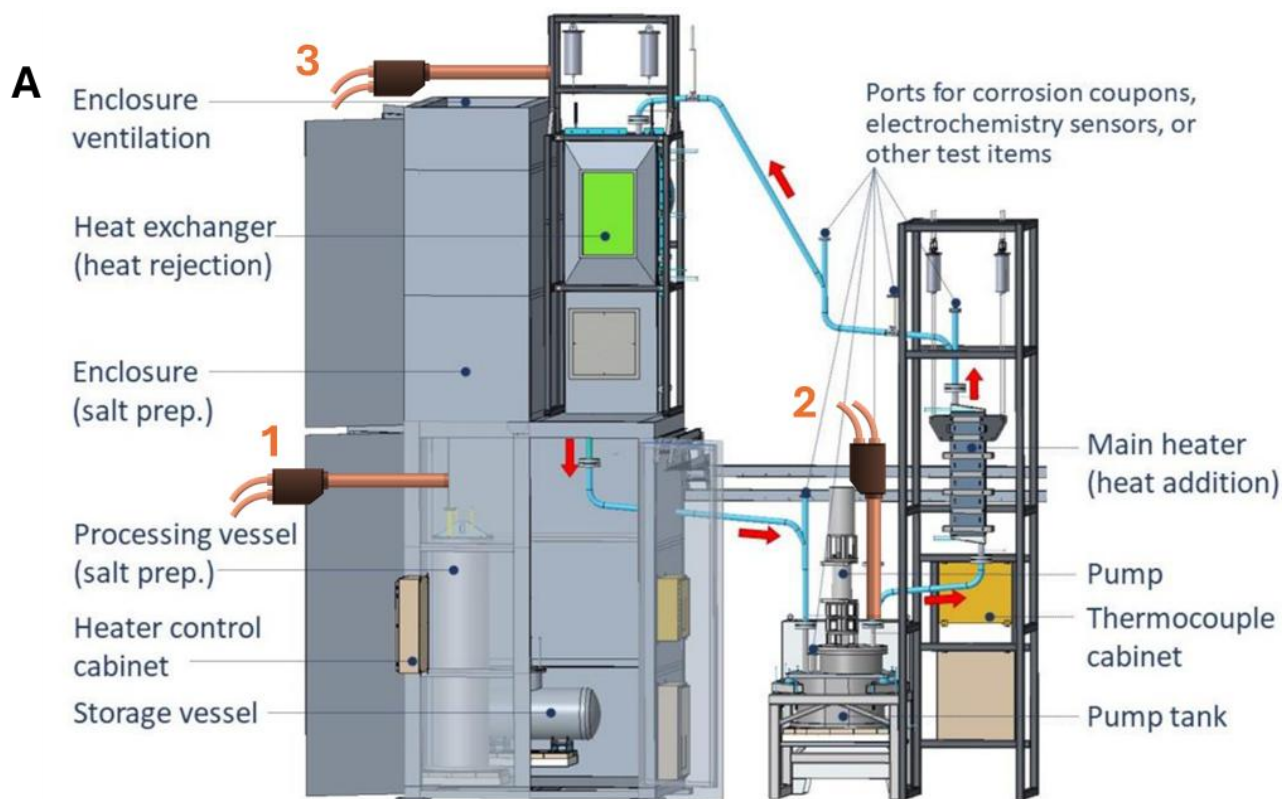


Figure 10. A) Schematic of FASTR adapted from a previous report¹⁶ with Raman probe locations indicated in orange (not to scale). Photos of locations where Raman probes were incorporated into the FASTR loop are shown in B) salt storage tank, C) pump tank, D) top of the manifold.

The first experiment performed involved sparging the salt storage tank with 4% H_2 in Ar followed by 4% D_2 in Ar. In this experiment, a Raman probe was inserted above the salt storage tank (Figure 10B) on a gas outlet line and the results are shown in Figure 11. Throughout this experiment, H_2 and D_2 were alternated with Ar gas at increasing sparging gas flow rates shown in Figure 11E. The Raman probe was able to detect H_2 and then D_2 with peak intensities

increasing with gas flow rates as gas concentration in the headspace of the salt storage tank increased. The Raman region where HD would be expected (3630 cm^{-1}) is plotted but no discernable signal was observed. It is important to note that with this probe, there was a peak at $\sim 3650\text{ cm}^{-1}$ that was present in all spectra. This signal could be caused by probe materials or gas line materials but its presence in all spectra indicates that it is not a gas phase analyte peak.

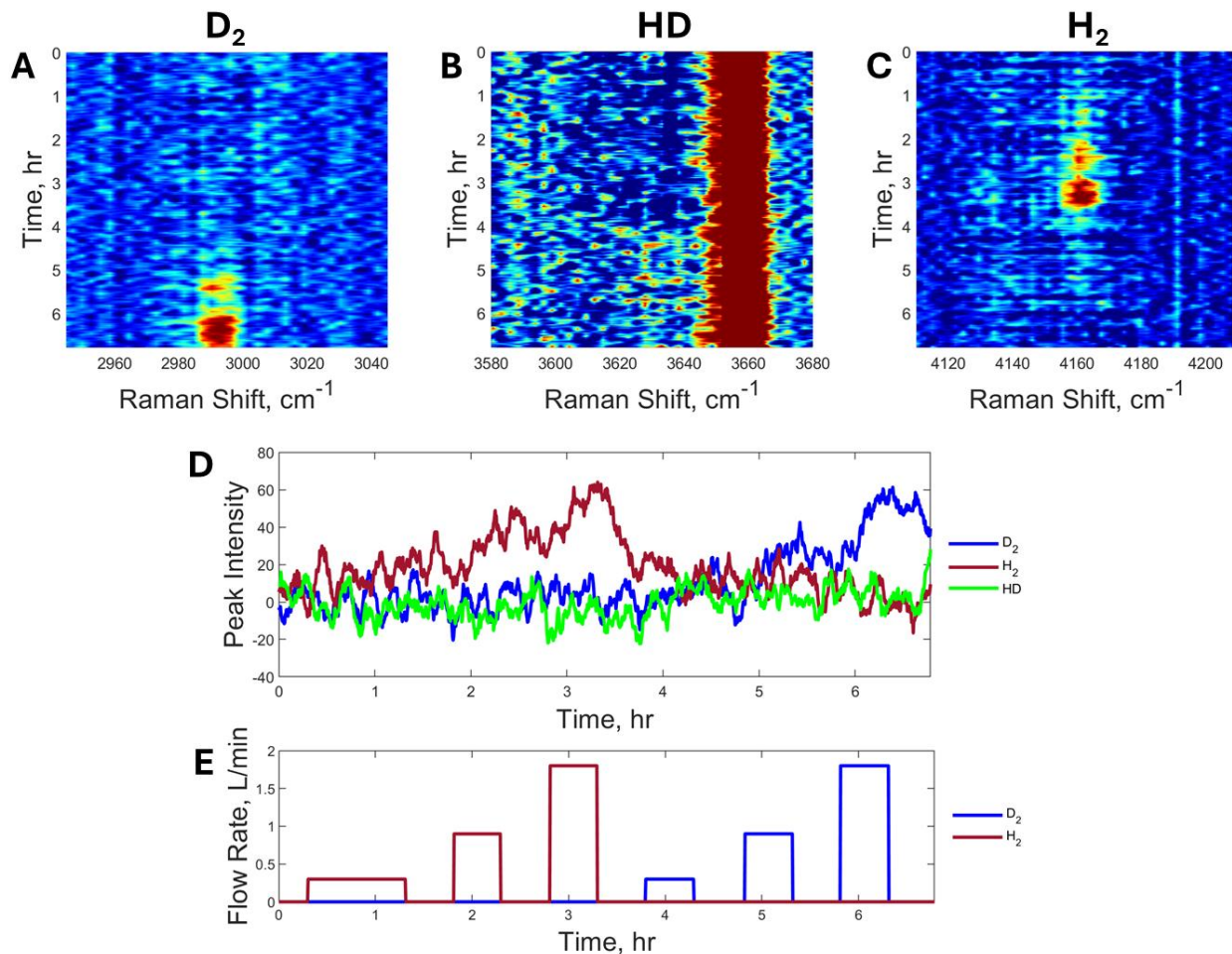


Figure 11. Top-down surface plots of Raman spectra measured on the Raman probe above the salt storage tank highlighting the A) D_2 region, B) HD region, and C) H_2 region. D) Peak intensities for D_2 , HD, and H_2 . E) Flow rates of H_2 and D_2 gas sparging. Spectra were averaged using a moving mean of 19 points.

The second experiment incorporated the gas flow cell in addition to the Raman probe above the salt storage tank to measure gas from the headspace above the salt storage tank. A gas sampling tube was inserted into the headspace of the salt storage tank. The Raman, LIBS, and RGA sampled gas from this line in tandem. Photos of the instrumentation and measurement cells are shown in Figure 12.

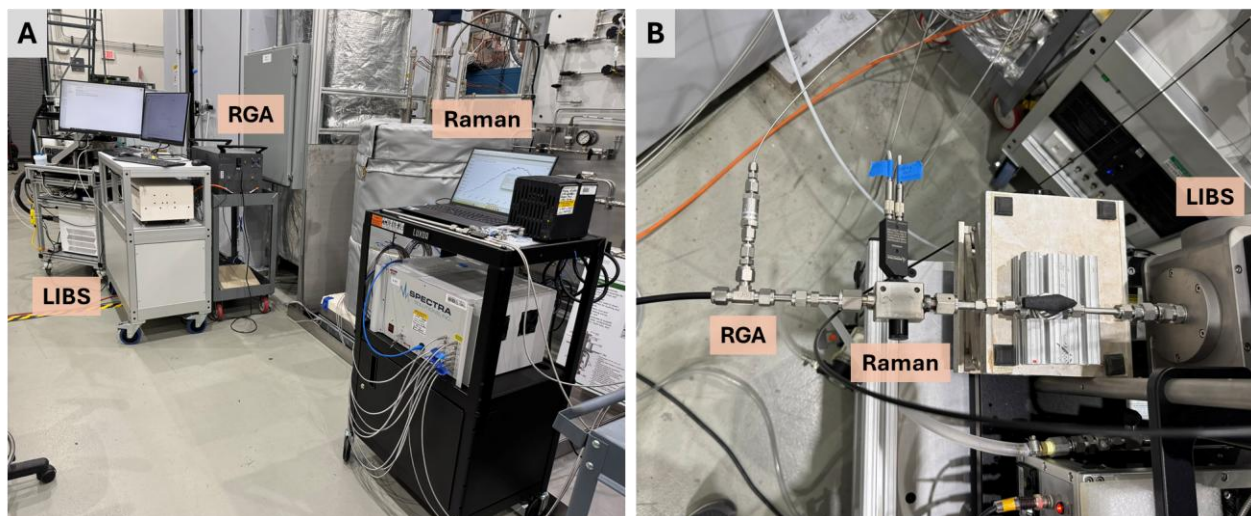


Figure 12. A) LIBS, RGA, and Raman instrumentation arranged for simultaneous measurements. B) Sampling of gas line from salt storage tank for simultaneous RGA, Raman, and LIBS measurements.

The results of this second experiment are shown in Figure 13 for the Raman probe (pictured in Figure 10B) and in Figure 14 for the gas flow cell (pictured in Figure 12B). For measurements collected at each location, D_2 and H_2 were both detected after the start of each gas flow and the flow rate correlates to the peak intensity. This is especially seen in Figure 13D-E and Figure 14D-E between hours 6 and 7 where the H_2 gas pressure was lowered and then increased. The H_2 peak intensity also drops with the decrease in gas flow rate and increases when the gas flow rate increases. Both Raman sensors also appeared to detect the formation of HD. There was a slight increase in a peak around 3630 cm^{-1} consistent with the location of HD.¹⁷ This peak appeared at the point where the gases were switched between D_2 and H_2 and would be at the time with the highest concentration of both gases in the system.

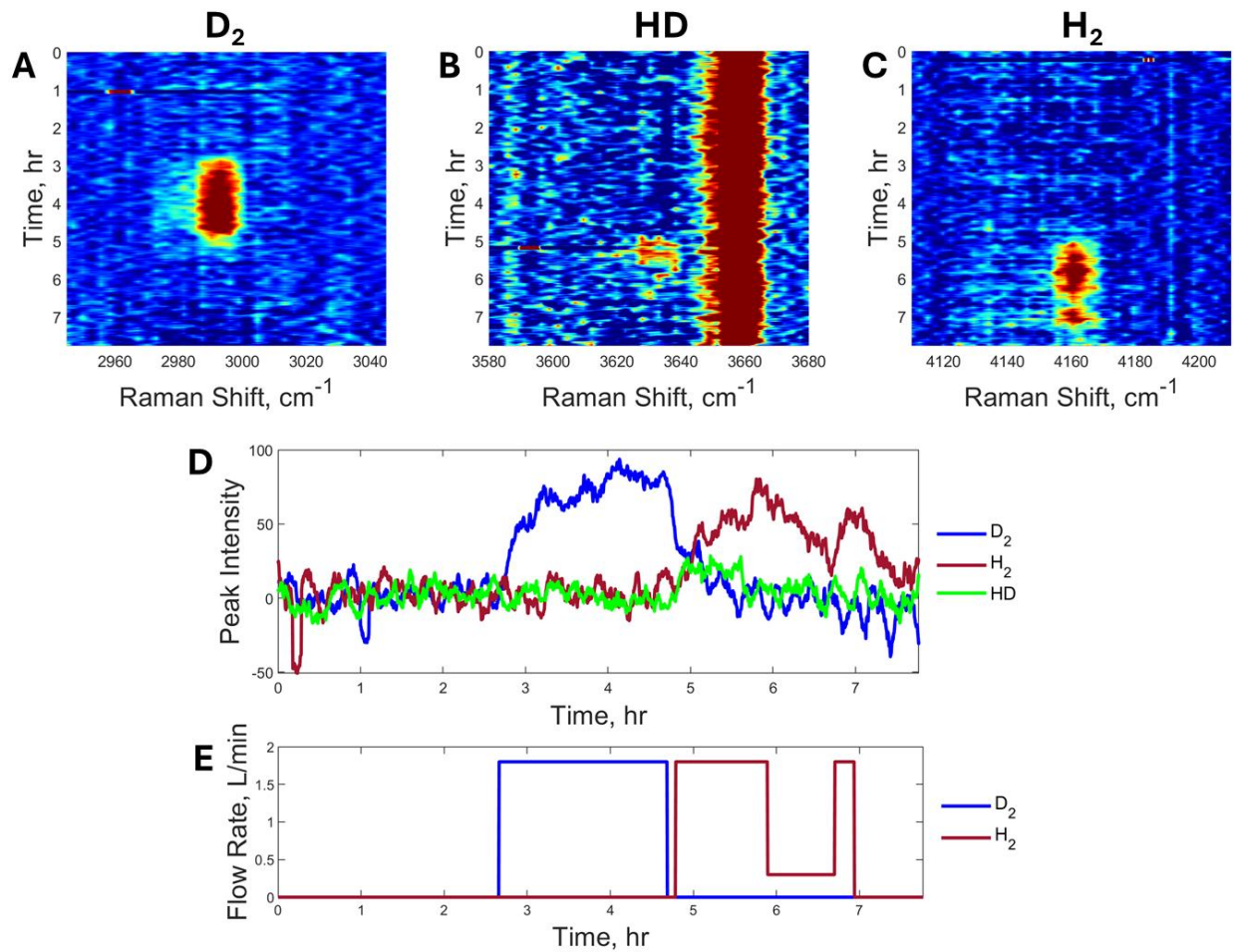


Figure 13. Top-down surface plots of Raman spectra collected on the Raman probe above the salt storage tank highlighting the A) D_2 region, B) HD region, and C) H_2 region. D) Peak intensities for D_2 , HD, and H_2 . E) Flow rates of H_2 and D_2 gas sparging. Spectra were averaged using a moving mean of 19 points.

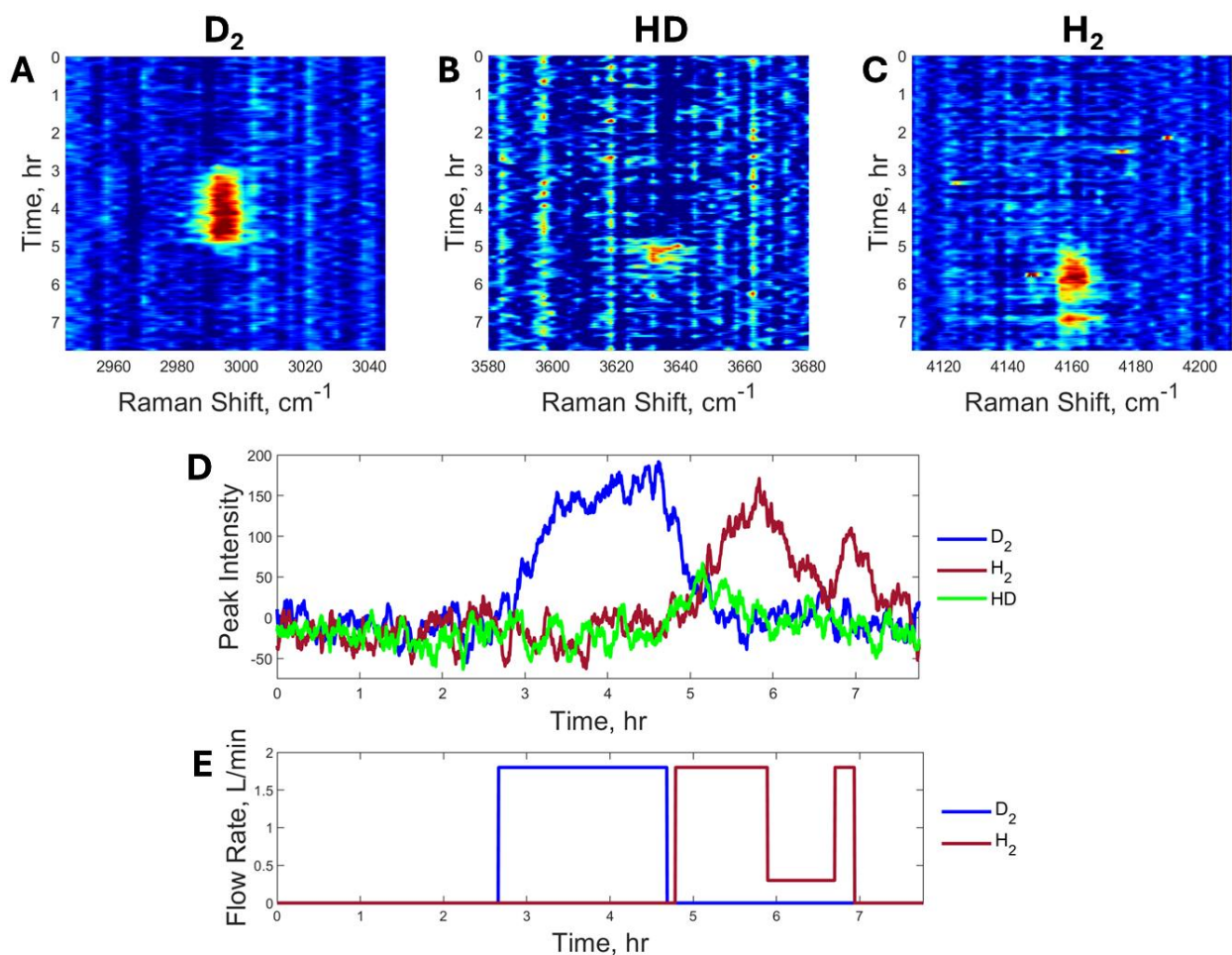


Figure 14. Top-down surface plots of Raman spectra collected on the gas flow cell highlighting the A) D_2 region, B) HD region, and C) H_2 region. D) Peak intensities for D_2 , HD, and H_2 . E) Flow rates of H_2 and D_2 gas sparging. Spectra were averaged using a moving mean of 19 points.

Throughout these experiments, LIBS was able to measure H and D peaks and monitor the peak intensities as a function of gas flow rate. LIBS will be more sensitive to the concentration of H and D than the Raman system used in this work, but as an elemental measurement, LIBS will be unable to differentiate between molecular species. The H and D peaks also overlap in LIBS and require a high-resolution instrument to differentiate between the two isotopes. RGA was also able to detect H_2 , D_2 , and HD during these experiments, though without higher resolution, the RGA would be unable to differentiate between molecules of similar masses such as HD and tritium. Raman can distinguish between all molecular hydrogen isotopologues but is limited by the sensitivity of the measurements. This is why combining multiple sensors is so valuable. Combining Raman, LIBS, and RGA, allows for not only the quantification of species present, but also the determination of molecular speciation. Data analysis and collaboration between the PNNL and ORNL teams will continue to compare and correlate the results of all systems.

4.0 Conclusions and recommendations

The PNNL focus for FY25 was to demonstrate two key advancements:

- 1) Optimization of a Raman sensor flow cell for low concentration gas-phase applications
- 2) Collaborative demonstration of Raman integration on operating salt loop to collect data in concert with other sensors

In the case of optimizing flow cells, the PNNL team optimized the sensor design to improve limits of detection, particularly in connection with optimized instrumentation while streamlining the footprint of the sensor. Results show desired improvements in sensitivity; a key item of note was the testing and demonstration of the novel sensor design on the active salt loop at ORNL.

In the case of collaborative demonstration, PNNL worked closely with ORNL to complete an on-site integration of Raman sensors onto an operating salt loop. PNNL provided 4 sensors (3 traditional Raman probes and the gas flow cell) which were integrated into the loop by the ORNL team. Data was collected simultaneously on multiple Raman probes while LIBS and RGA sensors were also operating on the loop. Gas composition was modified through the introduction of H_2 and D_2 into the loop. Results indicated good Raman performance and complementary output between the various sensors. Next steps include returning probes to PNNL for analysis of materials degradation and teams are considering collaborative sharing of information.

Moving forward, extended demonstration of sensor performance on active salt loops as well as extension to include and integrate additional sensing modalities is needed. Tools such as data fusion may be a pathway to build out highly robust and automated approaches to characterizing off-gas streams.

5.0 References

- (1) Riley, B. J.; McFarlane, J.; DelCul, G. D.; Vienna, J. D.; Contescu, C. I.; Forsberg, C. W. Molten salt reactor waste and effluent management strategies: A review. *Nuclear Engineering and Design* 2019, 345, 94-109. DOI: 10.1016/j.nucengdes.2019.02.002.
- (2) Riley, B.; McFarlane, J.; Del Cul, G.; Vienna, J. D.; Contescu, C. I.; Hay, L. M.; Savino, A. V.; Adkins, H. *Identification of Potential Waste Processing and Waste Form Options for Molten Salt Reactors*; Oak Ridge National Lab.(ORNL), Oak Ridge, TN (United States), 2018.
- (3) McFarlane, J.; Ezell, N.; Del Cul, G.; Holcomb, D. E.; Myhre, K.; Chapel, A.; Lines, A.; Bryan, S.; Felmy, H. M.; Riley, B. *Fission Product Volatility and Off-Gas Systems for Molten Salt Reactors*; Oak Ridge National Lab.(ORNL), Oak Ridge, TN (United States), 2019.
- (4) Felmy, H. M.; Cox, R. M.; Espley, A. F.; Campbell, E. L.; Kersten, B. R.; Lackey, H. E.; Branch, S. D.; Bryan, S. A.; Lines, A. M. Quantification of Hydrogen Isotopes Utilizing Raman Spectroscopy Paired with Chemometric Analysis for Application across Multiple Systems. *Anal Chem* 2024, 96 (18), 7220-7230. DOI: 10.1021/acs.analchem.4c00802.
- (5) Felmy, H. M.; Clifford, A. J.; Medina, A. S.; Cox, R. M.; Wilson, J. M.; Lines, A. M.; Bryan, S. A. On-Line Monitoring of Gas-Phase Molecular Iodine Using Raman and Fluorescence Spectroscopy Paired with Chemometric Analysis. DOI: 10.1021/acs.est.0c06137.
- (6) Andrews, H. B.; Kitzhaber, Z. B.; Orea, D.; McFarlane, J. Real-Time Elemental and Isotopic Measurements of Molten Salt Systems through Laser-Induced Breakdown Spectroscopy. DOI: 10.1021/jacs.4c13684.
- (7) Andrews, H. B.; Kitzhaber, Z. B.; McFarlane, J. Real-time monitoring of trace noble gases using laser-induced breakdown spectroscopy-An investigation of the impact of bulk gas on plasma properties and sensitivity. *Spectrochim Acta B* 2025, 230. 10.1016/j.sab.2025.107237.
- (8) Kitzhaber, Z. B.; Orea, D.; McFarlane, J.; Manard, B. T.; Andrews, H. B. Spurge Sampling of Molten Salts for Online Monitoring via Laser-Induced Breakdown Spectroscopy. *Acs Omega* 2025. DOI: 10.1021/acsomega.5c04988.
- (9) Hughey, K. D.; Bradley, A. M.; Tonkyn, R. G.; Felmy, H. M.; Blake, T. A.; Bryan, S. A.; Johnson, T. J.; Lines, A. M. Absolute Band Intensity of the Iodine Monochloride Fundamental Mode for Infrared Sensing and Quantitative Analysis. *The Journal of Physical Chemistry A* 2020. DOI: 10.1021/acs.jpca.0c07353.
- (10) Felmy, H. M.; Clifford, A. J.; Medina, A. S.; Cox, R. M.; Wilson, J. M.; Lines, A. M.; Bryan, S. A. On-Line Monitoring of Gas-Phase Molecular Iodine Using Raman and Fluorescence Spectroscopy Paired with Chemometric Analysis. *Environmental Science & Technology* 2021. DOI: 10.1021/acs.est.0c06137.
- (11) Felmy, H. M.; Cox, R. M.; Espley, A. F.; Campbell, E. L.; Kersten, B. R.; Lackey, H. E.; Branch, S. D.; Bryan, S. A.; Lines, A. M. Quantification of Hydrogen Isotopes Utilizing Raman Spectroscopy Paired with Chemometric Analysis for Application across Multiple Systems. *Analytical Chemistry* 2024, 96 (18), 7220-7230. DOI: 10.1021/acs.analchem.4c00802.
- (12) Bryan, S. A.; Levitskaia, T. G.; Lines, A. M.; Smith, F. N.; Josephson, G. B.; Bello, J. M. Dual-Remote Raman Technology for In-Situ Identification of Tank Waste. In WM Symposia 2013: International Collaboration and Continuous Improvement, Phoenix, Arizona; 2013.
- (13) Felmy, H. M.; Cox, R. M.; Lines, A. M.; Bryan, S. A. *Demonstration of Optical Spectroscopic Online Monitoring for Molten Salt Reactor Off-Gas Streams*; PNNL- 36645; Pacific Northwest National Laboratory, Richland, WA (United States), 2024.
- (14) Andrews, H. B.; Kitzhaber, Z. B.; Orea, D.; McFarlane, J. Real-Time Elemental and Isotopic Measurements of Molten Salt Systems through Laser-Induced Breakdown Spectroscopy. DOI: 10.1021/jacs.4c13684.

- (15) Kitzhaber, Z. B.; Orea, D.; McFarlane, J.; Manard, B. T.; Andrews, H. B. Sparge Sampling of Molten Salts for Online Monitoring via Laser-Induced Breakdown Spectroscopy. *ACS Omega* 2025, *10* (33), 37889-37897. DOI: 10.1021/acsomega.5c04988.
- (16) Robb, K.; Baird, S.; Massengale, J.; Kappes, E.; Mulligan, P. L. *Facility to Alleviate Salt Technology Risks (FASTR): Design Report*; Oak Ridge National Laboratory (ORNL), Oak Ridge, TN (United States), 2022.
- (17) Veirs, D. K.; Rosenblatt, G. M. Raman line positions in molecular hydrogen: H₂, HD, HT, D₂, DT, and T₂. *Journal of Molecular Spectroscopy* 1987, *121* (2), 401-419. DOI: 10.1016/0022-2852(87)90058-0.

Pacific Northwest National Laboratory

902 Battelle Boulevard
P.O. Box 999
Richland, WA 99354

1-888-375-PNNL (7665)

www.pnnl.gov